Microscopic restoration of proton-neutron mixed symmetry in weakly collective nuclei

J. D. Holt,[1,2,*] N. Pietralla,[1,3,4] J. W. Holt,[1] T. T. S. Kuo,[1] and G. Rainovski[1]
[1]*Department of Physics and Astronomy, SUNY, Stony Brook, New York 11794-3800, USA*
[2]*TRIUMF, 4004 Wesbrook Mall, Vancouver, British Columbia V6T 2A3, Canada*
[3]*Institut für Kernphysik, Technische Universität Darmstadt, D-64289 Darmstadt, Germany*
[4]*Institut für Kernphysik, Universität zu Köln, D-50937 Köln, Germany*
(Received 7 September 2006; revised manuscript received 28 June 2007; published 27 September 2007)

Starting from the microscopic low-momentum nucleon-nucleon interaction $V_{\mathrm{low}\,k}$, we present a systematic shell-model study of magnetic moments and magnetic dipole transition strengths of the basic low-energy one-quadrupole phonon excitations in nearly spherical nuclei. Studying in particular the even-even $N = 52$ isotones from ^{92}Zr to ^{100}Cd, we find the predicted evolution of the predominantly proton-neutron nonsymmetric state reveals a restoration of collective proton-neutron mixed-symmetry structure near midshell. This provides a quantitative explanation for the existence of pronounced collective mixed-symmetry structures in weakly collective nuclei.

DOI: 10.1103/PhysRevC.76.034325 PACS number(s): 21.10.Re, 21.30.Fe, 21.60.Cs, 27.60.+j

Mesoscopic quantum systems such as Bose-Einstein condensates, superconductors, and quark-gluon systems are some of the most intensely studied in contemporary physics [1,2]. Their dynamical properties are determined by the interplay and mutual balance of collective and single-particle degrees of freedom. In two fluid systems such as atomic nuclei, the presence of an isospin degree of freedom serves only to enhance this complexity. Of particular interest for understanding the physics of these systems is the microscopic origin of those excitations possessing collective two-fluid character. Collective quadrupole isovector excitations in the valence shell, so-called mixed-symmetry states (MSSs) [3], are the best-studied examples of this class of excitations. A special type of MSS, the 1^+ scissor mode, was predicted to exist [4] and discovered [5] in atomic nuclei. It is not surprising, then, that analogous scissor-mode states have subsequently been found in other two-fluid quantum systems such as trapped Bose-Einstein condensed gases [6,7], metallic clusters [8], and elliptical quantum dots [9].

Even though MSSs are a common feature of two-fluid quantum systems, atomic nuclei are still the primary laboratory in which our understanding of them can be shaped. In the interacting boson model of heavy nuclei (IBM-2) the definition of MSSs is formalized by the bosonic F-spin symmetry [3]. It arises predominantly from a collective coupling of proton and neutron subsystems, and when the proton/neutron (pn) valence spaces are large enough, strong coupling can arise between them. Naturally, then, the best examples of pn-symmetric and MSSs would be expected at midshells. However, pronounced MSSs have recently also been observed in weakly collective nuclei especially in the $N = 52$ isotones. Multiphonon structures of MSSs are observed in the nucleus ^{94}Mo [10–12], in neighboring nuclei [13–15], and recently the first MSSs in an odd-mass nearly-spherical nucleus were identified in ^{93}Nb [16]. The experimental properties of MSSs in this region have already been described within the framework of the IBM-2 [17,18], the nuclear shell model (SM) [14,19], and the quasiparticle-phonon model [20]. Although the mechanism describing how symmetric and MS structures appear has been discussed by Heyde and Sau [21] in a schematic way, the question of how these states systematically evolve has not yet been addressed in a quantitative microscopic approach.

In this article, we provide a microscopic foundation for the formation and evolution of the fundamental MSS of vibrational nuclei, the one-quadrupole phonon $2^+_{1,\mathrm{ms}}$ state, from SM calculations using the low-momentum nucleon-nucleon (NN) interaction $V_{\mathrm{low}\,k}$ [22]. $V_{\mathrm{low}\,k}$ defines a new class of NN interaction with a variable momentum cutoff (or resolution scale) that reproduces low-energy two-nucleon observables. Shell-model calculations using $V_{\mathrm{low}\,k}$ with a fixed cutoff, have already been used successfully in recent nuclear structure studies, e.g., Ref. [23]. For $N = 52$ isotones from the $Z = 40$ to the $Z = 50$ shell closures, we here investigate the structure and electromagnetic properties of the two SM 2^+ states with predominant one-phonon character (labeled 2^+_I and 2^+_{II}), where the 2^+_{II} state is connected to the 2^+_I state by a strong $M1$ transition. The 2^+_I and 2^+_{II} SM states with large seniority-2 components are interpreted as the experimentally observed one-phonon symmetric 2^+_1 and mixed symmetric $2^+_{1,\mathrm{ms}}$ states, respectively. The evolution of these states is seen by examining two of the most important observables: $B(M1; 2^+_{II} \to 2^+_I)$ values and the magnetic moments of the 2^+_I and 2^+_{II} states. Our calculations indicate that the quantity driving this evolution is the orbital proton contribution to the $M1$ transitions. Moreover, the main cause underlying the formation of MSSs in these weakly collective nuclei is the approximate energy degeneracy in the proton and the neutron one-phonon quadrupole excitations. This mechanism can be considered as a *microscopic restoration of proton-neutron symmetry*. Because of the universal nature of MS states, these studies should serve as qualitative predictions of MS formation and structural evolution in other nuclear regions, and give parallel insight into analogous structures in general mesoscopic quantum systems.

*jholt@triumf.ca

 ©2007 The American Physical Society

Our microscopic shell-model calculations are based on the low-momentum NN interaction $V_{\mathrm{low}\,k}$. Although various NN potentials have been developed that reproduce the NN data up to momenta of ~ 2 fm^{-1} [24], they differ in their treatment of the high-momentum modes, which are known to complicate many-body calculations. Using the renormalization group, we start from one of the high-precision interactions and integrate out the high-momentum components above a cutoff Λ such that the physics below this cutoff is preserved. It has been shown that as Λ is lowered to 2.1 fm^{-1}, the $V_{\mathrm{low}\,k}$ interactions flow to a result largely independent of the input interaction [22,25]. Furthermore, $V_{\mathrm{low}\,k}$ is energy independent and thus suitable for SM calculations in any nuclear region [26]. For the present work we use a $V_{\mathrm{low}\,k}$ interaction derived from the CD-Bonn [27] potential with a cutoff $\Lambda = 2.1$ fm^{-1}. Using the two-body matrix elements of $V_{\mathrm{low}\,k}$, we then derive a SM effective interaction V_{eff} based on the folded diagram methods detailed in Ref. [28]. Through this process we include the effects of core polarization to second order, which has been shown to be a reasonable approximation to all order effects in the absence of many-body interactions [29].

The present calculations were carried out with the OXBASH code [30] using the effective interaction described above. ^{88}Sr was used as the inert core and the proton-neutron model space taken to be: $\pi : [2p_{1/2}, 1g_{9/2}]$ and $\nu : [1g_{7/2}, 2d_{5/2}, 2d_{3/2}, 3s_{1/2}, 1h_{11/2}]$, where the single particle energies were taken from the experimental values in ^{89}Sr and ^{89}Y, as shown in Table I. We have verified the validity of this procedure through extensive comparison with experimental data in ^{92}Zr, ^{94}Mo, and ^{96}Ru [31], as well as the prediction of the properties of MSSs in the odd-mass nearly-spherical nucleus ^{93}Nb [16,31]. It is debatable whether or not the ^{88}Sr core is suitable for such calculations due to the close proximity of both the $2p_{3/2}$ and the $1f_{5/2}$ proton orbits. We should emphasize, however, that our goal is not a highly accurate reproduction of experimental data, but to understand global features of MSSs in terms of this model space.

The key experimental signature for MSSs is a strong $M1$ transition from the 2_1^+ to the $2^+_{1,\mathrm{ms}}$ state, due to the isovector character of the $M1$ operator. The strength and fragmentation of this transition is an indicator of the purity of the MSSs. Bare orbital gyromagnetic factors $g_\pi^l = 1\mu_N$, $g_\nu^l = 0$, with empirical (but not fine-tuned to fit the data) spin factors $g_\pi^s = 3.18\mu_N$, and $g_\nu^s = -2.18\mu_N$ were used (as in Ref. [19]). These values result in a pure isovector spin $M1$ operator, which simplifies the interpretation. The calculated $B(M1)$ values

TABLE I. Single-particle energies for the orbits used in our shell-model calculations.

Proton orbits:					
	$p_{1/2}$	$g_{9/2}$			
Energy (MeV)	−0.91	0.0			
Neutron orbits:					
	$g_{7/2}$	$d_{5/2}$	$d_{3/2}$	$s_{1/2}$	$h_{11/2}$
Energy (MeV)	1.47	0.0	2.01	1.03	3.00

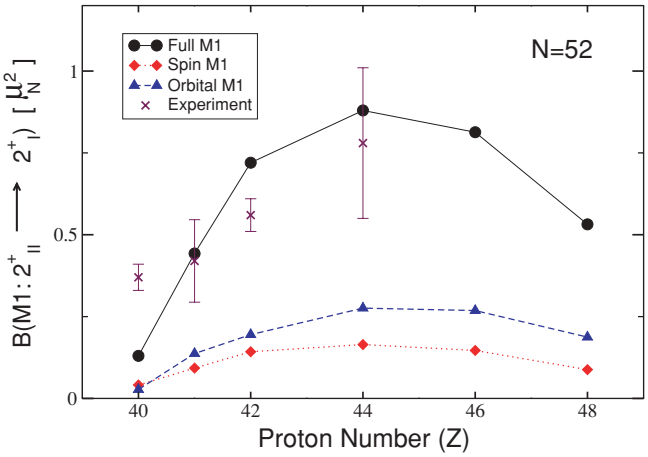

FIG. 1. (Color online) Evolution of the total, orbital, and spin $B(M1; 2^+_{II} \to 2^+_I)$ values for $N = 52$ isotones. The experimental values are from Refs. [12,13,15,16].

shown in Fig. 1. They show a pronounced parabolic behavior, maximized at mid-subshell. Also plotted in Fig. 1 are the spin and orbital contributions, both exhibiting an approximately parabolic shape.

The increase in $M1$ strength from ^{92}Zr to ^{96}Ru is in good qualitative agreement with the data, though the SM calculations underpredict the value in ^{92}Zr and somewhat overpredict it in ^{94}Mo. In Fig. 1, for comparison purposes, we have also included the *average* value of the $M1$ transitions from the mixed-symmetry doublet states, $\frac{5}{2}^-_{\mathrm{ms}}$ $\frac{3}{2}^-_{\mathrm{ms}}$, to the like-$J$ one-phonon states in ^{93}Nb [16]; it is clearly in general agreement with the overall trend. For ^{98}Pd and ^{100}Cd, however, a decrease in $M1$ strength is predicted—indicating less purely collective excitations.

Figure 2 shows the predicted evolution of the g factors of the 2_I^+ and 2_{II}^+ states. As proton number increases the 2_I^+ g factors increase almost linearly, whereas the 2_{II}^+

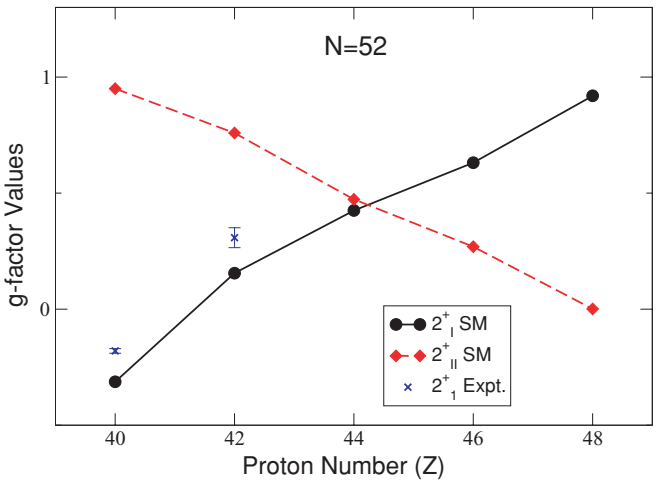

FIG. 2. (Color online) Predicted evolution of the g factors for the 2_I^+ and 2_{II}^+ states across the series of $N = 52$ isotones. The experimental values are from Refs. [32,33].

g factors decrease linearly with approximately the same absolute slope. As a result they cross at midshell. The calculated g factors in ^{96}Ru for the 2^+_I and 2^+_{II} states are close (0.42 and 0.48, respectively) and not far from the $Z/A = 0.458$ value expected for a fully collective state with pn symmetry. The negative g factor (-0.31) predicted for the 2^+_I state in ^{92}Zr is in qualitative agreement with experiment [14,32], indicating significant neutron character of this state. At $Z = 40$ the 2^+_I state of ^{92}Zr is expected to be primarily neutron in character. In drastic contrast, we predict a large positive g factor for the 2^+_{II} state in ^{92}Zr, which suggests a dominant proton character, from the $J = 2$ coupling of protons in the $\pi(g^2_{9/2})$ orbit. As discussed in Ref. [14], the unbalanced proton-neutron content of the ^{92}Zr 2^+_I and 2^+_{II} states implies severe breaking of F-spin symmetry, not a surprise for such a weakly collective system. This phenomenon where we see varying contributions to the one-phonon states by the active proton and neutron particles due to subshell structure can be interpreted as *configuration-isospin polarization* (CIP). Significant CIP corresponds to a breaking of the F-spin symmetry in the IBM-2, which is reflected in the small $M1$ transition strength (see Fig. 1), while vanishing CIP indicates a restoration of F-spin symmetry and pure FS/MS states. The changes in the $M1$ strengths and the g factors for the 2^+_I and 2^+_{II} states from ^{92}Zr to ^{100}Cd isotopes consistently show the evolution of CIP, and hence pn symmetry character, of these states: the purity of the MS character of the 2^+_{II} state peaks in the midshell region, where CIP vanishes, before waning at the approach of the $Z = 50$ shell closure, where CIP increases again.

The p/n orbit/spin contributions to the $M1$ matrix elements, $\langle 2^+_i \| g^{l,s}_{\pi,\nu} \cdot (M1)^{l,s}_{\pi,\nu} \| 2^+_i \rangle_{(i=I,II)}$ are shown in Fig. 3. Considering first the 2^+_I states, we see that in ^{92}Zr, the neutron-spin $(g^s_\nu \cdot M1^s_\nu)$ component dominates, resulting in the negative g factor. In ^{94}Mo, however, the $M1^l_\pi$ contribution has risen, whereas the $M1^s_\nu$ has declined, yielding a small and slightly positive g factor. For the rest of the isotones, the $M1^l_\pi$ component continues increasing, whereas the others become more negligible. For the 2^+_{II} states, the opposite situation is seen due to the orthogonality of this one-phonon state to the

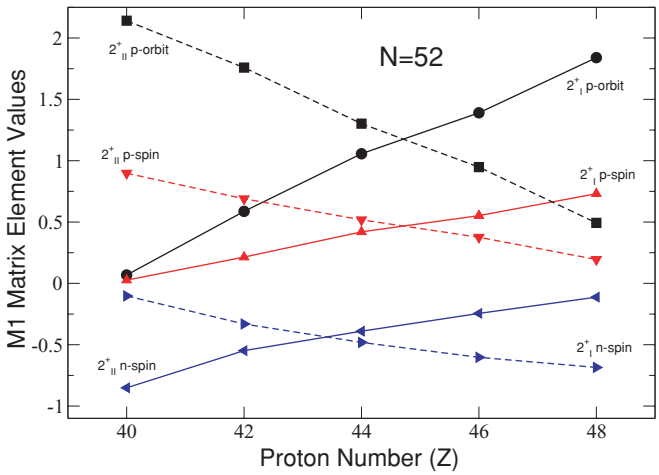

FIG. 3. (Color online) Calculated proton/neutron orbital/spin matrix elements contributing to the g factors.

TABLE II. Amplitudes of the dominant SM configurations contributing to the $J^\pi = 2^+$ one-phonon wave functions.

Nucleus	Wave function components	2^+_I	2^+_{II}
^{92}Zr	$\pi(g^2_{9/2})_0\ \nu(d^2_{5/2})_2$	0.462	−0.129
	$\pi(g^2_{9/2})_2\ \nu(d^2_{5/2})_0$	0.078	0.725
^{94}Mo	$\pi(p^2_{1/2}g^2_{9/2})_0\ \nu(d^2_{5/2})_2$	0.682	−0.461
	$\pi(p^2_{1/2}g^2_{9/2})_2\ \nu(d^2_{5/2})_0$	0.426	0.652
^{96}Ru	$\pi(p^2_{1/2}g^4_{9/2})_0\ \nu(d^2_{5/2})_2$	0.586	−0.584
	$\pi(p^2_{1/2}g^4_{9/2})_2\ \nu(d^2_{5/2})_0$	0.512	0.548
^{98}Pd	$\pi(p^2_{1/2}g^6_{9/2})_0\ \nu(d^2_{5/2})_2$	0.510	−0.681
	$\pi(p^2_{1/2}g^6_{9/2})_2\ \nu(d^2_{5/2})_0$	0.576	0.448
^{100}Cd	$\pi(p^2_{1/2}g^8_{9/2})_0\ \nu(d^2_{5/2})_2$	0.376	−0.787
	$\pi(p^2_{1/2}g^8_{9/2})_2\ \nu(d^2_{5/2})_0$	0.638	0.305

2^+_I state. The $M1^l_\pi$ term remains the driving force behind the evolution of the g factor, starting at a large, positive value in ^{92}Zr. It remains dominant until near $Z = 50$ where it has decreased to near zero, whereas the $M1^s_\nu$ element has become negative enough to influence the g factor. The observed prominence of the orbital matrix element further confirms the collective nature of these excitations.

The calculated SM wave functions are generally complicated, but as discussed in [19], MS structure is evident in the dominant components. Table II gives the dominant amplitudes for the normalized 2^+_I and 2^+_{II} wave functions. With the exception of the 2^+_I state in ^{92}Zr, the significant contributions come from the $\pi(p^2_{1/2}g^k_{9/2})_0\nu(d^2_{5/2})_2$ and $\pi(p^2_{1/2}g^k_{9/2})_2\nu(d^2_{5/2})_0$ configurations, where $k = 2$ for ^{94}Mo, $k = 8$ for ^{100}Cd, and the protons are jointly coupled to either $J = 0$ or $J = 2$. For ^{92}Zr we have only listed the $\pi(g^2_{9/2})\nu(d^2_{5/2})$ configuration because the two protons in $\pi(p^2_{1/2})$ cannot couple to $J = 2$. These components represent only a part of the full wave functions, but the percentage is typically on the order of 60 to 70%. From Table II we see that the dominant parts of the 2^+_I and 2^+_{II} wave functions generally exhibit a pn-symmetric structure. Even with these drastically truncated wave functions, the 2^+_I and 2^+_{II} are formed by the same dominant components and are approximately orthogonal: we find $\langle 2^+_I | 2^+_{II} \rangle < 0.1$ in every case. The evolution of the $M1$ strength and the g factors is apparent—at the low end of the isotone chain, the CIP is strong such that the 2^+_I state is predominantly neutron in character and the 2^+_{II} state is largely proton. In ^{94}Mo already both components are more equally important. For the 2^+_I state, there is a linear increase in proton character and decrease in neutron character across the shell with the opposite behavior seen in the 2^+_{II} states. At midshell in ^{96}Ru, where the CIP approximately vanishes, both states have almost equal absolute amplitude of proton and neutron excitations forming the fully symmetric and mixed symmetry one-quadrupole phonon states.

These approximated wave functions and their $M1$ matrix elements can be considered in the seniority scheme. The proton and neutron contributions to the predominant seniority-two ($\nu = 2$) parts of the one-quadrupole phonon wave functions in this sequence of isotones can be related to the fractional

filling $f = (Z - 40)/10$ of the $\pi(g_{9/2})$ orbital with protons. The wave functions can be empirically approximated as

$$|2_I^+\rangle \approx \sqrt{f}|2_\pi^+\rangle + \sqrt{1-f}|2_\nu^+\rangle$$
$$|2_{II}^+\rangle \approx \sqrt{1-f}|2_\pi^+\rangle - \sqrt{f}|2_\nu^+\rangle, \quad (1)$$

where the $|2^+_{\pi(\nu)}\rangle$ represents a SM configuration in which the protons (neutrons) are coupled to 2^+ and the neutrons (protons) are coupled to 0^+. To the extent that this two-state decomposition represents a large percentage of the total wave functions, we can deduce

$$g(2_I^+) = \sqrt{\frac{2\pi}{45}}\,[\mu_\nu + f(\mu_\pi - \mu_\nu)] \quad (2)$$

$$g(2_{II}^+) = \sqrt{\frac{2\pi}{45}}\,[\mu_\pi - f(\mu_\pi - \mu_\nu)] \quad (3)$$

$$B(M1; 2_{II}^+ \to 2_I^+) = \frac{1}{5} f(1-f)(\mu_\pi - \mu_\nu)^2 \quad (4)$$

with $\mu_{\pi(\nu)} = \langle 2^+_{\pi(\nu)} \| M1 \| 2^+_{\pi(\nu)} \rangle$ being the diagonal $M1$ matrix elements of the $\nu = 2$ proton (neutron) 2^+ configuration. Note that $\mu_\nu < 0$ is a constant for the $N = 52$ isotones and, within the seniority scheme, the matrix element $\mu_\pi > 0$ is independent of the filling of the proton orbital and, hence, a constant as well. It immediately follows that the g factor of the 2_I^+ state increases linearly with the filling of the $\pi(g_{9/2})$ orbital, whereas the g factor of the 2_{II}^+ state linearly drops, instead, with the same absolute slope. In contrast to this, the $M1$ transition strength is proportional to the factor $f(1-f)$ and exhibits a parabolic collective behavior over the $\pi(g_{9/2})$ shell with a maximum at midshell. The size of the $B(M1; 2_{II}^+ \to 2_I^+)$ value is proportional to the quadratic slope of the g factors. This relation is quantitatively $(\mu_\pi - \mu_\nu \approx 4.2\,\mu_N)$ in good agreement even with the full calculations.

Finally, the shell-model results are qualitatively at variance with the F-spin limit of the IBM-2. With effective boson g factors $g_\rho \equiv \sqrt{2\pi/45}\,\mu_\rho$ the predictions of the F-spin limit of the U(5) dynamical symmetry limit are

$$g(2_1^+) = \sqrt{\frac{2\pi}{45}}\left[\mu_\nu + \frac{N_\pi}{N}(\mu_\pi - \mu_\nu)\right]$$

$$g(2_{1,\mathrm{ms}}^+) = \sqrt{\frac{2\pi}{45}}\left[\mu_\pi - \frac{N_\pi}{N}(\mu_\pi - \mu_\nu)\right]$$

$$B(M1; 2_{1,\mathrm{ms}}^+ \to 2_1^+) = \frac{1}{5}\frac{N_\pi}{N}\left(1 - \frac{N_\pi}{N}\right)(\mu_\pi - \mu_\nu)^2,$$

which is formally identical to Eqs. (2)–(4) with the replacement $f \to N_\pi/N$ and $2_I^+ = 2_1^+, 2_{II}^+ = 2_{1,\mathrm{ms}}^+$. However, due to the convention of counting bosons as half of the number of valence particles or holes outside the nearest closed shell, the boson number fraction N_π/N does not correspond to the fractional filling f of the proton shell but is instead for $N_\nu = 1$ approximately equal to the fractional half-filling. The F-spin limit of the IBM-2 together with the conventional counting of bosons would lead to local extrema for the g factors of the one-phonon 2^+ states at midshell [maximum for $g(2_1^+)$ and minimum for $g(2_{1,\mathrm{ms}}^+)$] and to a reduction of the $B(M1; 2_{1,\mathrm{ms}}^+ \to 2_1^+)$ value from ^{94}Mo to ^{96}Ru in contradiction to the data. We note that a similar result is obtained when considering the F-spin limit in $O(6)$ symmetry, which has been argued to be the more appropriate IBM-2 dynamical symmetry in some of these nuclei [34].

The discrepancy in predicted evolution between the F-spin limit of the IBM-2 and the SM calculation using $V_{\mathrm{low}\,k}$ originates from the breaking of F-spin symmetry by CIP due to the subshell structure and the specific restoration of F-spin near midshell in the shell model. The F-spin limit is most fragile when the valence spaces are small and hence the degree of collectivity is low. Differences in excitation modes for protons and neutrons then easily lead to CIP of the low-energy wave functions and thus to a breaking of F-spin symmetry. There are two possibilities for restoring the F-spin limit. This can happen either when the valence spaces are large and the pn-coupling is strong or when the proton and neutron excitation modes are degenerate. In the second case even comparatively low collectivity in small valence spaces can lead to fully pn-symmetric or mixed-symmetric configurations. The SM signatures indicating CIP of the 2_I^+ and 2_{II}^+ states (the $M1 : 2_{II}^+ \to 2_I^+$ transition strength, the g factors, and the amplitude of the proton/neutron character of the wave functions) also indicate the degree to which F-spin is broken or restored. The smooth change in the proton-neutron character of the 2_I^+ and 2_{II}^+ states, evident from Table II, can be attributed to the variation of energies of the one-phonon proton and neutron configurations with filling of the $\pi(g_{9/2})$ orbital. This can be seen in the data for the semiclosed shell nuclei in the vicinity of the $N = 52$ isotones. The 2_1^+ energy of the even $N = 50$ isotones is indicative of the energy of the 2_π^+ excitation. It drops slightly from 1509 keV in ^{92}Mo to 1394 keV in ^{98}Cd. However, the energies of 2_1^+ states in the ^{92}Zr and ^{102}Sn are indicative of the energy of the 2_ν^+ excitation. The data increase from 934 keV in ^{92}Zr to 1472 keV in ^{102}Sn. The difference in energy of these basic $2^+_{\pi(\nu)}$ excitations translates into the IBM-2 framework in a difference of proton and neutron d-boson energies that cause a breaking of F-spin symmetry. Due to the low collectivity near shell closure, this breaking cannot be restored by strong pn coupling. As a result, F-spin breaking is most pronounced in ^{92}Zr [15] and must be expected for ^{100}Cd, too. The energy crossing of the 2_π^+ and 2_ν^+ configurations near midshell, where the collectivity also peaks (see Table II), causes a specific restoration of F-spin symmetry, yielding there the largest $B(M1)$ values and almost equal g factors. This process is microscopic in origin and differs from the usual F-spin symmetry generation due to the collective pn coupling in the framework of the IBM-2.

In summary we have used the low-momentum NN interaction $V_{\mathrm{low}\,k}$ to provide a microscopic description of the evolution of MSSs and magnetic dipole collectivity—studying the $N = 52$ isotones as a particular example. The predicted observables reveal a new specific restoration of proton-neutron symmetry that originates from the energy degeneracy of basic proton and neutron excitations. This process offers for the first time an explanation for the existence of pronounced $2_{1,\mathrm{ms}}^+$

structures in weakly collective nuclei and might be observable in other two-fluid quantum systems.

We thank B. A. Brown for his invaluable assistance with the Oxbash code and Ch. Stoyanov for enlightening discussions. Support from the U.S. Department of Energy under contract DE-FG02-88ER40388, the Natural Sciences and Engineering Research Council of Canada (NSERC), and from the German DFG under grant number SFB 634 is gratefully acknowledged. TRIUMF receives federal funding via a contribution agreement through the National Research Council of Canada.

[1] W. Ketterle, Rev. Mod. Phys. **74**, 1131 (2002).
[2] V. L. Ginzburg, Rev. Mod. Phys. **76**, 981 (2004).
[3] F. Iachello, Phys. Rev. Lett. **53**, 1427 (1984).
[4] N. Lo Iudice and F. Palumbo, Phys. Rev. Lett. **41**, 1532 (1978).
[5] D. Bohle, A. Richter, W. Steffen, A. E. L. Dieperink, N. Lo Iudice, F. Palumbo, and O. Scholten, Phys. Lett. **B137**, 27 (1984).
[6] D. Guéry-Odelin and S. Stringari, Phys. Rev. Lett. **83**, 4452 (1999).
[7] O. M. Maragó, S. A. Hopkins, J. Arlt, E. Hodby, G. Hechenblaikner, and C. J. Foot, Phys. Rev. Lett. **84**, 2056 (2000).
[8] V. O. Nesterenko, W. Kleinig, F. F. de Souza Cruz, and N. Lo Iudice, Phys. Rev. Lett. **83**, 57 (1999).
[9] L. Serra, A. Puente, and E. Lipparini, Phys. Rev. B **60**, R13 966 (1999).
[10] N. Pietralla, C. Fransen, D. Belic, P. von Brentano, C. Friessner, U. Kneissl, A. Linnemann, A. Nord, H. H. Pitz, T. Otsuka, I. Schneider, V. Werner, and I. Wiedenhöver, Phys. Rev. Lett. **83**, 1303 (1999).
[11] N. Pietralla, C. Fransen, P. von Brentano, A. Dewald, A. Fitzler, C. Friessner, and J. Gableske, Phys. Rev. Lett. **84**, 3775 (2000).
[12] C. Fransen, N. Pietralla, Z. Ammar, D. Bandyopadhyay, N. Boukharouba, P. von Brentano, A. Dewald, J. Gableske, A. Gade, J. Jolie, U. Kneissl, S. R. Lesher, A. F. Lisetskiy, M. T. McEllistrem, M. Merrick, H. H. Pitz, N. Warr, V. Werner, and S. W. Yates, Phys. Rev. C **67**, 024307 (2003).
[13] N. Pietralla, C. J. Barton III, R. Krücken, C. W. Beausang, M. A. Caprio, R. F. Casten, J. R. Cooper, A. A. Hecht, H. Newman, J. R. Novak, and N. V. Zamfir, Phys. Rev. C **64**, 031301(R) (2001).
[14] V. Werner, D. Belic, P. von Brentano, C. Fransen, A. Gade, H. von Garrel, J. Jolie, U. Kneissl, C. Kohstall, A. Linnemann, A. F. Lisetskiy, N. Pietralla, H. H. Pitz, M. Scheck, K.-H. Speidel, F. Stedile, and S. W. Yates, Phys. Lett. **B550**, 140 (2002).
[15] C. Fransen, V. Werner, D. Bandyopadhyay, N. Boukharouba, S. R. Lesher, M. T. McEllistrem, J. Jolie, N. Pietralla, P. von Brentano, and S. W. Yates, Phys. Rev. C **71**, 054304 (2005).
[16] J. N. Orce, J. D. Holt, A. Linnemann, C. J. McKay, S. R. Lesher, C. Fransen, J. W. Holt, A. Kumar, N. Warr, V. Werner, J. Jolie, T. T. S. Kuo, M. T. McEllistrem, N. Pietralla, and S. W. Yates, Phys. Rev. Lett. **97**, 062504 (2006).
[17] F. Iachello and A. Arima, *The Interacting Boson Model* (Oxford University Press, New York, 1990).
[18] P. van Isacker, K. Heyde, J. Jolie, and A Sevrin, Ann. Phys. (NY) **171**, 253 (1986).
[19] A. F. Lisetskiy, N. Pietralla, C. Fransen, R. V. Jolos, and P. von Brentano, Nucl. Phys. **A677**, 100 (2000).
[20] N. Lo Iudice and Ch. Stoyanov, Phys. Rev. C **62**, 047302 (2000); **65**, 064304 (2002); **69**, 044312 (2004); **73**, 037305 (2006).
[21] K. Heyde and J. Sau, Phys. Rev. C **33**, 1050 (1986).
[22] S. K. Bogner, T. T. S. Kuo, and A. Schwenk, Phys. Rep. **386**, 1 (2003).
[23] L. Coraggio, A. Covello, A. Gargano, and N. Itaco, Phys. Rev. C **70**, 034310 (2004); **72**, 057302 (2005); **73**, 031302(R) (2006).
[24] R. Machleidt and I. Slaus, J. Phys. G **27**, R69 (2001).
[25] S. K. Bogner, T. T. S. Kuo, A. Schwenk, D. R. Entem, and R. Machleidt, Phys. Lett. **B576**, 265 (2003).
[26] S. K. Bogner, T. T. S. Kuo, L. Coraggio, A. Covello, and N. Itaco, Phys. Rev. C **65**, 051301(R) (2002).
[27] R. Machleidt, Phys. Rev. C **63**, 024001 (2001).
[28] T. T. S. Kuo and E. Osnes, *Lecture Notes in Physics* (Springer-Verlag, New York, 1990), Vol. 364.
[29] J. D. Holt, J. W. Holt, T. T. S. Kuo, G. E. Brown, and S. K. Bogner, Phys. Rev. C **72**, 041304(R) (2005).
[30] B. A. Brown, A. Etchegoyen, N. S. Godwin, W. D. M. Rae, W. A. Richter, W. E. Ormand, E. K. Warburton, J. S. Winfield, L. Zhao, and C. H. Zimmerman, MSU-NSCL report number 1289.
[31] J. D. Holt *et al.* (in preparation).
[32] J. Jakob, N. Benczer-Koller, J. Holden, G. Kumbartzki, T. J. Mertzimekis, K.-H. Speidel, C. W. Beausang, and R. Krücken, Phys. Lett. **B468**, 13 (1999).
[33] P. F. Mantica, A. E. Stuchbery, D. E. Groh, J. I. Prisciandaro, and M. P. Robinson, Phys. Rev. C **63**, 034312 (2001).
[34] N. A. Smirnova, N. Pietralla, A. Leviatan, J. N. Ginocchio, and C. Fransen, Phys. Rev. C **65**, 024319 (2002).